

Report for exercise 4 from group A

Tasks addressed: 5

Authors:
 Hirmay Sandesara (03807348)
 Yikun Hao (03768321)
 Yusuf Alptigin Gün (03796825)
 Subodh Pokhrel (03796731)
 Atahan Yakici (17065009)

Last compiled: 2025-06-24

The work on tasks was divided in the following way:

Hirmay Sandesara (03807348)	Task 1	20%
	Task 2	20%
	Task 3	20%
	Task 4	20%
	Task 5	20%
Yikun Hao (03768321)	Task 1	20%
	Task 2	20%
	Task 3	20%
	Task 4	20%
	Task 5	20%
Yusuf Alptigin Gün (03796825)	Task 1	20%
	Task 2	20%
	Task 3	20%
	Task 4	20%
	Task 5	20%
Subodh Pokhrel (03796731)	Task 1	20%
	Task 2	20%
	Task 3	20%
	Task 4	20%
	Task 5	20%
Atahan Yakici (17065009)	Task 1	20%
	Task 2	20%
	Task 3	20%
	Task 4	20%
	Task 5	20%

1 Vector Fields, Orbits, and Visualization

In this task, we visualized the qualitative behavior of different linear dynamical systems in two dimensions. The goal was to reproduce all topologically distinct types of hyperbolic equilibria — such as nodes, saddles, and foci — by varying a single parameter in a family of linear systems. Each phase portrait was generated for a specific choice of parameter α , and classified according to the sign and type of the system's eigenvalues.

Setup: We used two separate parameterized matrix families to generate all required behaviors:

- To produce **nodes** and the **saddle**, we used:

$$A = \begin{bmatrix} \alpha & 0 \\ 0 & \alpha + 2 \end{bmatrix}$$

- To generate **spiral sinks/sources** and the **center**, we used:

$$A = \begin{bmatrix} \alpha & -2 \\ 2 & \alpha \end{bmatrix}$$

Phase portraits. Figure 1 shows six phase portraits generated using these matrix families. Each system corresponds to a different qualitative class and is annotated with its eigenvalues. The classification based on the number of eigenvalues with positive (n_+) and negative (n_-) real parts is as follows:

- **Stable Node:** $\alpha = -3.0$
Eigenvalues real and negative $\Rightarrow (n_+, n_-) = (0, 2)$
- **Stable Focus:** $\alpha = -1.0$
Complex eigenvalues with negative real part $\Rightarrow (n_+, n_-) = (0, 2)$
- **Saddle:** $\alpha = -1.0$
Real eigenvalues of opposite sign $\Rightarrow (n_+, n_-) = (1, 1)$
- **Center:** $\alpha = 0.0$
Purely imaginary eigenvalues \Rightarrow not hyperbolic (excluded from classification)
- **Unstable Node:** $\alpha = 1.0$
Eigenvalues real and positive $\Rightarrow (n_+, n_-) = (2, 0)$
- **Unstable Focus:** $\alpha = 1.0$
Complex eigenvalues with positive real part $\Rightarrow (n_+, n_-) = (2, 0)$

Topological equivalence: According to the classification of hyperbolic fixed points, systems that share the same pair (n_+, n_-) are topologically equivalent — that is, they have qualitatively the same phase portrait under a homeomorphism preserving time orientation:

- The **stable node** and **stable focus** are topologically equivalent since both have $(0, 2)$.
- The **unstable node** and **unstable focus** are topologically equivalent with $(2, 0)$.
- The **saddle** with $(1, 1)$ is in its own unique topological class.
- The **center** is not hyperbolic (zero real part) and thus excluded from this classification.

In order to visualize, the code was written in Python using a modular structure and proper documentation. Visualization was done using `matplotlib.streamplot`, and eigenvalues were computed using NumPy. Each phase portrait was labeled with its classification and eigenvalues automatically.

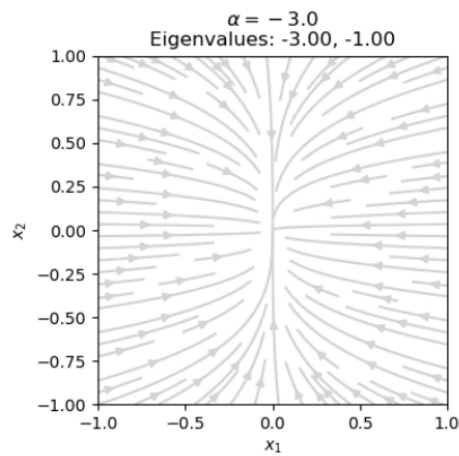
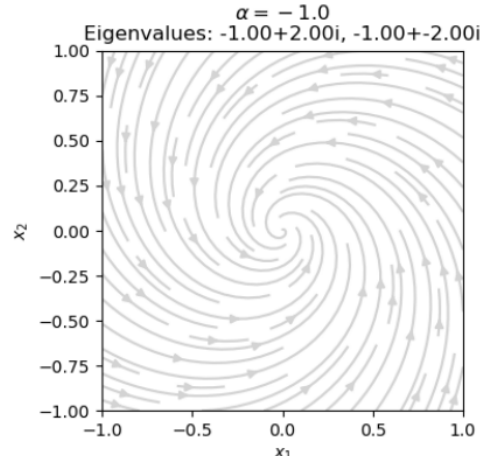
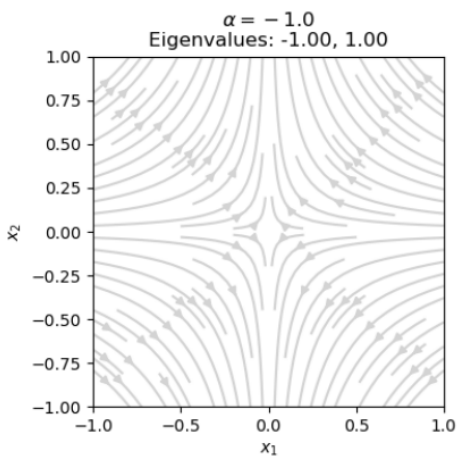
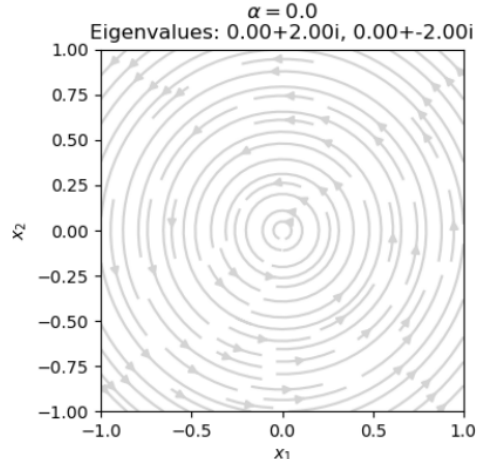
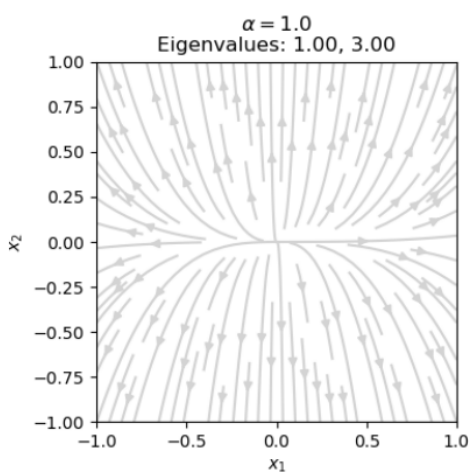
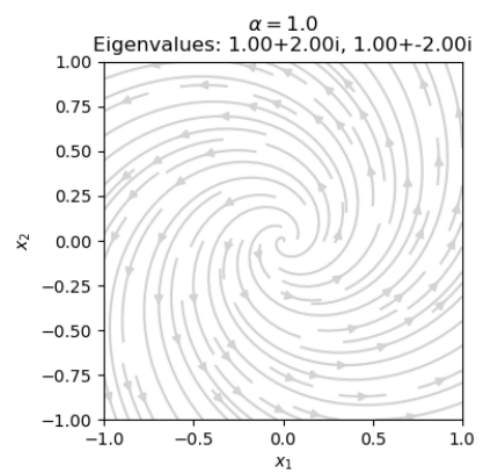
**Stable Node** ($n_+ = 0, n_- = 2$)**Stable Focus** ($n_+ = 0, n_- = 2$)**Saddle** ($n_+ = 1, n_- = 1$)**Center** (non-hyperbolic)**Unstable Node** ($n_+ = 2, n_- = 0$)**Unstable Focus** ($n_+ = 2, n_- = 0$)

Figure 1: Phase portraits categorized by the number of eigenvalues with positive (n_+) and negative (n_-) real parts. Systems with the same (n_+, n_-) are topologically equivalent.

2 Common Bifurcations in Nonlinear Systems

In this section, we analyze two 1D nonlinear dynamical systems with a single parameter α . Our goal is to identify the type of bifurcation that occurs. We visualise it with bifurcation diagrams and discuss the topological equivalence and normal form of the systems. The two systems under consideration are:

$$\dot{x} = \alpha - x^2 \quad (1)$$

$$\dot{x} = \alpha - 2x^2 - 3 \quad (2)$$

Our analysis is supported by Python and Jupyter Notebook scripts, which compute the steady states and their stability. They generate the corresponding bifurcation diagrams. The Jupyter Notebook `task2.ipynb` plots the bifurcation graphs by using `plot_bifurcation_1d` from `utils.py`, which uses Task21 and Task22 from `dynamical_system.py` as input.

2.1 Analysis of System (1): $\dot{x} = \alpha - x^2$

In our first system, governed by Equation 1, the steady states (or fixed points) are found by setting the time derivative to zero: $\dot{x} = 0$.

$$\alpha - x^2 = 0 \implies x^* = \pm\sqrt{\alpha}$$

Nature of the steady states depends on the parameter α :

- For the case when $\alpha < 0$, there are no real solutions for x^* . Hence, our system has no steady states.
- For the case when $\alpha = 0$, there is a single steady state at $x^* = 0$.
- For $\alpha > 0$, there are two distinct steady states at $x^* = \pm\sqrt{\alpha}$.

At our critical parameter value, which is $\alpha = 0$; the system's qualitative behavior changes. Two steady states are created where there were none before. This type of bifurcation is known as a ‘saddle-node bifurcation’ [5].

2.1.1 Stability Analysis

The stability of the steady states is given by the sign of the derivative of the vector field (f'). That is in our case, $f(x) = \alpha - x^2$, evaluated at the steady state. The derivative is $f'(x) = -2x$.

- For the case when our steady state $x^* = +\sqrt{\alpha}$ (where $\alpha > 0$), the derivative is $f'(+\sqrt{\alpha}) = -2\sqrt{\alpha} < 0$. A negative derivative indicates that this is a *stable* steady state (essentially a node).
- For the case when our steady state $x^* = -\sqrt{\alpha}$ (where $\alpha > 0$), the derivative is $f'(-\sqrt{\alpha}) = 2\sqrt{\alpha} > 0$. A positive derivative indicates that this is an *unstable* steady state (essentially a saddle).

Our plotted bifurcation diagram in Figure 2a visually represents this particular analysis. The x-axis is the parameter α , and the y-axis is the state variable x . Stable steady states are shown with a dotted blue line, and unstable ones with a dotted red line, clearly illustrating the saddle-node bifurcation at $\alpha = 0$.

2.2 Analysis of our system (2): $\dot{x} = \alpha - 2x^2 - 3$

For our second system, as described by Equation 2. We follow the same analysis. Setting $\dot{x} = 0$ yields:

$$\alpha - 2x^2 - 3 = 0 \implies x^* = \pm\sqrt{\frac{\alpha - 3}{2}}$$

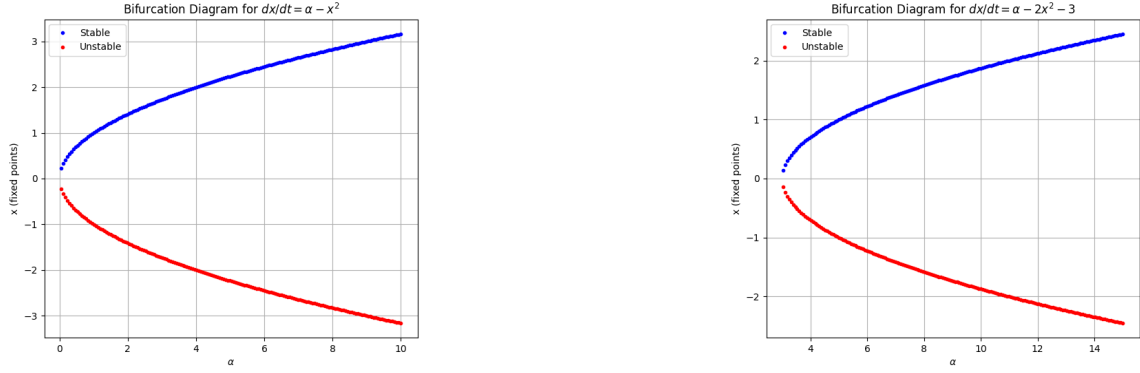
Real solutions for x^* exist only if $\alpha - 3 \geq 0$, which means $\alpha \geq 3$. Thus, our system undergoes a “saddle-node bifurcation” at the critical parameter value $\alpha_c = 3$.

2.2.1 Stability Analysis

The stability is determined by the derivative $f'(x) = -4x$.

- For $x^* = +\sqrt{(\alpha - 3)/2}$ (where $\alpha > 3$), $f'(x^*) < 0$, so this is a *stable* steady state.
- For $x^* = -\sqrt{(\alpha - 3)/2}$ (where $\alpha > 3$), $f'(x^*) > 0$, so this is an *unstable* steady state.

This behavior is depicted in the bifurcation diagram in Figure 17(b).



(a) Bifurcation diagram for $\dot{x} = \alpha - x^2$. A saddle-node bifurcation occurs at $\alpha = 0$.

(b) Bifurcation diagram for $\dot{x} = \alpha - 2x^2 - 3$. A saddle-node bifurcation occurs at $\alpha = 3$.

Figure 2: Bifurcation diagrams for our two nonlinear systems. Stable steady states are plotted as (dotted) blue lines, while unstable steady states are plotted as (dotted) red lines. The plots visually confirm that both systems undergo a saddle-node bifurcation, albeit at different parameter values.

2.3 Topological Equivalence and Normal Form

2.3.1 Topological Equivalence

We can say that any two dynamical systems are topologically equivalent if there exists a 'homeomorphism' (also known as a topological isomorphism): a mapping that preserves all topological properties. Here, mapping the orbits of one system to the orbits of the other, preserving the direction of time. The number of fixed points is a topological invariant, so we want the same number of fixed points [1].

- At $\alpha = 1$: Our system (1) has two steady states at $x^* = \pm 1$. System (2) has no steady states, this is as $1 < 3$. Since the number of fixed points differs, the systems are **not topologically equivalent** at $\alpha = 1$.
- At $\alpha = -1$: Our system (1) has no steady states. Our system (2) also has no steady states (as $-1 < 3$). In both systems, \dot{x} is always negative. This means all trajectories flow from $+\infty$ to $-\infty$. Since there are no fixed points to distinguish the phase portraits, a simple homeomorphism (such as a scaling and translation) can map the orbits of one system to the other. Therefore, the systems are **topologically equivalent** at $\alpha = -1$.

2.3.2 Normal Form

Normal form of a bifurcation is the simplest mathematical representation that captures the main/essential dynamics near our bifurcation point [6]. We make an argument that both systems have the same normal form by showing they can be transformed into the same structure through a change of variables. The normal form for a saddle-node bifurcation is typically written as $\dot{y} = \mu \pm y^2$.

- Our system (1), $\dot{x} = \alpha - x^2$, is already in this normal form. With parameter $\mu = \alpha$ and state $y = x$.
- For our system (2), $\dot{x} = \alpha - 2x^2 - 3$, we introduce a new parameter $\mu = \alpha - 3$ to shift the bifurcation point to the origin. The equation becomes $\dot{x} = \mu - 2x^2$. Now, we can rescale the state variable by letting $y = \sqrt{2}x$, which means $dy = \sqrt{2}dx$. By putting this in as a substitution, we get:

$$\begin{aligned} \frac{1}{\sqrt{2}} \frac{dy}{dt} &= \mu - 2 \left(\frac{y}{\sqrt{2}} \right)^2 = \mu - y^2 \\ \Rightarrow \frac{dy}{dt} &= \sqrt{2}(\mu - y^2) \end{aligned} \tag{3}$$

By rescaling time with $\tau = \sqrt{2}t$. We arrive with the standard normal form $\frac{dy}{d\tau} = \mu - y^2$.

Since both systems can be reduced to the same canonical equation through simple transformations. We conclude that they belong to the same bifurcation class and share the same "saddle-node normal form".

3 Bifurcations in higher dimensions

3.1 Andronov-Hopf bifurcation

This section of the report deals with Task 3, where we explore bifurcations in two-dimensional dynamical systems, focusing on the Andronov–Hopf bifurcation. The system under investigation is given by the normal form:

$$\begin{aligned}\dot{x}_1 &= \alpha x_1 - x_2 - x_1(x_1^2 + x_2^2), \\ \dot{x}_2 &= x_1 + \alpha x_2 - x_2(x_1^2 + x_2^2).\end{aligned}\tag{4}$$

3.1.1 Varying α

We analyze how the behaviour of the system changes with the parameter α . The differences in the behaviour are visualized using phase portraits as seen in Figure 3

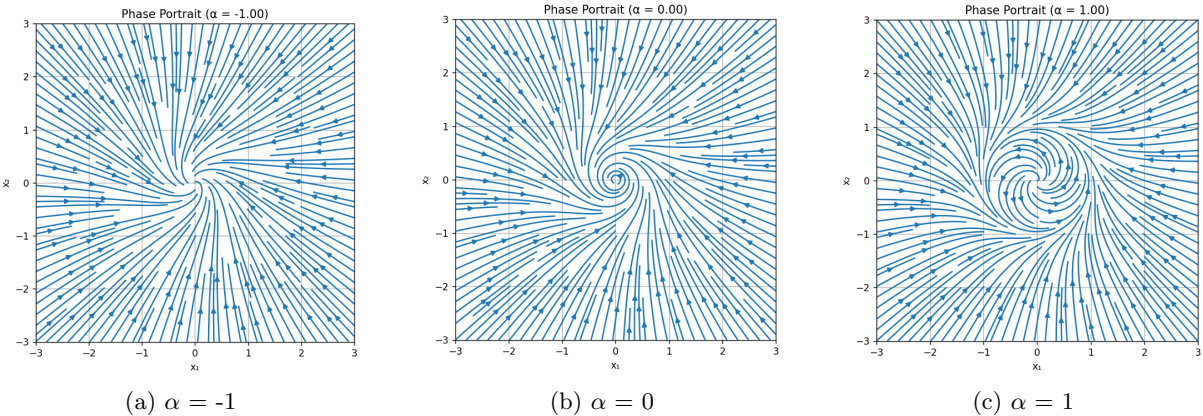


Figure 3: Phase portraits at different α values

The bifurcation behavior in Figure 3 shows plots for $\alpha = [-1, 0, 1]$ and these show:

- $\alpha = -1$: stable spiral towards origin
- $\alpha = 0$: bifurcation point, neutral center
- $\alpha = 1$: stable limit cycle

For the Andronov–Hopf bifurcation in a two-dimensional dynamical system with different α , it is seen that at $\alpha < 0$, the system has an asymptotically stable equilibrium point at the origin to which all trajectories spiral. At $\alpha = 0$, the origin is still the center, trajectories spiral in a circle around the origin, and it is the critical point of the Hopf bifurcation. For $\alpha > 0$, it is seen that the origin becomes unstable, but there is a spiral limit cycle around the origin.

3.1.2 Orbit Visualization for $\alpha = 1$

To further analyze the behavior of the system, we simulate numerically, two orbits of the system for $\alpha = 1$, starting at the initial conditions $(x_1, x_2) = (2, 0)$ and $(x_1, x_2) = (0.5, 0)$. The results are shown in Figure 4. The calculation of the orbits in a phase diagram is essentially solving a system of first-order ordinary differential equations (ODEs) numerically (in our case, using Euler's method).

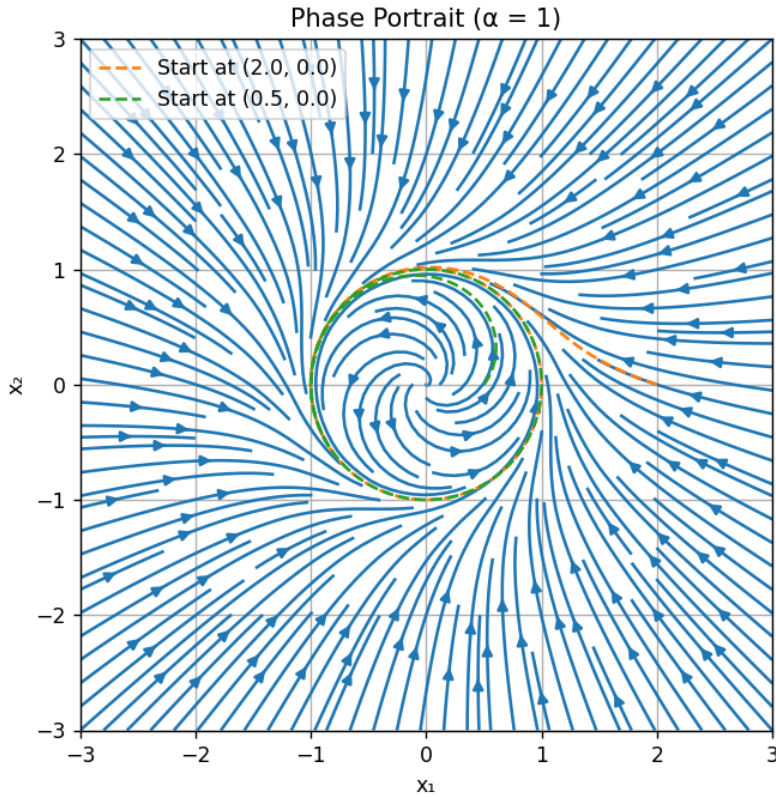


Figure 4: Phase portrait for $\alpha = 1$ with two trajectories: one starting at $(2.0, 0.0)$ and the other at $(0.5, 0.0)$.

Using the initial points, the Euler method is used to calculate the next point. This is done by the following equations:

$$\begin{aligned} x_1^{(n+1)} &= x_1^{(n)} + h \cdot (\alpha x_1^{(n)} - x_2^{(n)} - x_1^{(n)} ((x_1^{(n)})^2 + (x_2^{(n)})^2)), \\ x_2^{(n+1)} &= x_2^{(n)} + h \cdot (x_1^{(n)} + \alpha x_2^{(n)} - x_2^{(n)} ((x_1^{(n)})^2 + (x_2^{(n)})^2)), \end{aligned} \quad (5)$$

where h is a small time step (we used $h = 0.001$), and n the iteration step.

After a number of iterations, the trajectories, as shown in Figure 4, spiral toward a closed curve—the stable limit cycle—which confirms the typical behavior of a supercritical Hopf bifurcation:

- The orange dashed line shows the trajectory from the initial point $(2.0, 0.0)$. This shows an inward spiral until it reaches the stable state.
- The green dashed line shows the trajectory from $(0.5, 0.0)$, which spirals outward towards the same stable state.

Both converge to the same stable periodic orbit (limit cycle), demonstrating the system's long-term behavior at $\alpha = 1$.

3.2 Cusp bifurcation

In this section, we look at a bifurcation in one state space dimension $X = \mathbb{R}$, but with two parameters $\alpha \in \mathbb{R}^2$. This is the cusp bifurcation, and in Figure 5 we visualize the bifurcation surface (i.e. all points (x, α_1, α_2) where $\dot{x} = 0$) of the cusp bifurcation in a 3D plot for the normal form:

$$\dot{x} = \alpha_1 + \alpha_2 x - x^3 \quad (6)$$

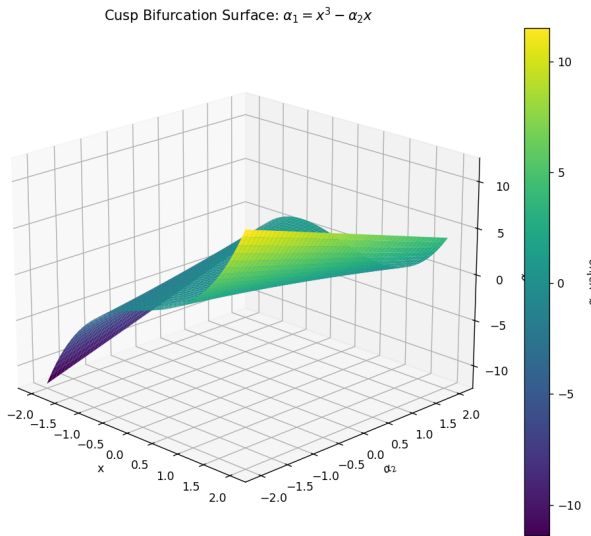


Figure 5: Cusp bifurcation surface

The image is obtained by sampling points (x, α_2) uniformly and then plotting the surface as a function of (x, α_2) .

In order to visualize the cusp location and shape easily, we project it into a 2-dimensional plot (known as the bifurcation set and lies in the (α_1, α_2) -plane. The result of this projection is seen in Figure 6.

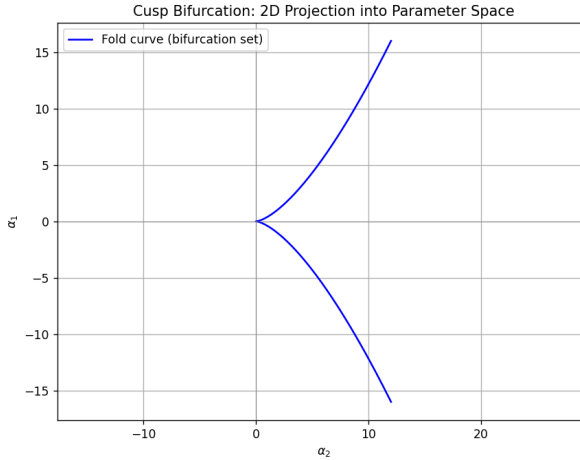
Figure 6: Projection of cusp to a (α_1, α_2) -plane

Figure 6 shows a simplified, 2D version of the 3D cusp bifurcation surface shown in Figure 5. Instead of the full surface shown by Figure 5 by plotting the variable α_1 as a function of x and α_2 , Figure 6 focuses only on the shape of the bifurcation in the parameter space (α_1, α_2) . In other words, Figure 6 shows the projection of the surface from Figure 5 onto the (α_1, α_2) -plane.

The curved lines in the 2D diagram indicate the critical values where the surface in Figure 6 folds. Inside this cusp-shaped region, the surface has three layers (corresponding to three real solutions), whereas outside of it, there is only one real solution.

4 Chaotic dynamics

4.1 Logistic Map

The task is to analyze the logistic map described by the discrete evaluation function:

$$x_{n+1} = rx_n(1 - x_n), n \in \mathbb{N} \quad (7)$$

with the parameter $r \in (0, 4]$ and $x \in [0, 1]$. We analyze its dynamics by examining its fixed points, bifurcations, and the overall bifurcation diagram as the parameter r is varied.

4.1.1 Fixed Point and Stability Analysis

Fixed point analysis is the basis of stability analysis and bifurcation analysis. A fixed point is called an equilibrium, and the evolution operator maps an equilibrium onto itself. Equivalently, a system placed at an equilibrium remains there forever[2]. The fixed points of the system, marked as x^* , are found by solving $x^* = f(x^*, r)$, here specifically

$$x^* = rx^*(1 - x^*), n \in \mathbb{N} \quad (8)$$

solving equation 8 yields two fixed points:

- $x^* = 0$
- $x^* = 1 - 1/r$

As the next step, the stability of the two result points is analyzed. When considering a discrete-time dynamical system $f(s)$, the Jacobian matrix of which denoted by A , the fixed point is stable if all eigenvalues $\mu_1, \mu_2, \dots, \mu_n$ of A satisfy $|\mu| < 1$. Here specifically, the discrete map only has one state variable x_n , and the system is classified as one-dimensional. Therefore, the Jacobian matrix is simplified to a 1×1 matrix, and is simply the derivative of itself. The system is stable if $|f'(x^*)| < 1$. Solve the equation 9:

$$f'(x) = \frac{d}{dx} rx(1 - x) = r - 2rx \quad (9)$$

Substitute $x^* = 0$ into the derivative expression, we obtain $|r| < 1$. Since we are investigating the range $r > 0$, the stable interval for this fixed point is $0 < r < 1$. Similarly, substitute $x^* = 1 - 1/r$ into the same derivative expression, we obtain $|2 - r| < 1$. This equals $1 < r < 3$. Until this step, we have derived the interval of convergence for each fixed point, and the result is the basis of bifurcation analysis.

4.1.2 Bifurcation Analysis

This section analyses the qualitative changes (bifurcations) in the logistic map's dynamics as the parameter r increases. As calculated in 4.1.1, the system has two fixed points, and each has its own interval of convergence. We vary r from 0 to 2 and from 2 to 4 separately.

1. Vary r from 0 to 2
For $r \in (0, 1)$, the system converges to a single fixed point $x^* = 0$. Then at $r = 1$, the steady state given by $x^* = 1 - 1/r$ begins to inherit the stability, while the fixed point $x^* = 0$ loses its stability. Therefore, a **transcritical bifurcation** occurs at this numerical value. That is to say, at the numerical value of $r = 1$, these two fixed points collide, exchange their stability, and then pass through each other. $r \in (1, 2)$, the system now has a single stable steady state at $x^* = 1 - 1/r$.
2. Vary r from 2 to 4
For $r \in [2, 3)$, the system continues to have the steady state at $x^* = 1 - 1/r$, and all trajectories converge to it. However, at $r = 3$, the steady state $x^* = 1 - 1/r$ becomes unstable. Then, the system oscillates between two distinct values, and a stable period of 2 cycles emerges as a parameter is varied. For $r \in (3, 4]$, the system bifurcates into a stable 4-cycle, followed by an 8-cycle, then 16, 32, 64, and so on with more and more reduced intervals of r .
3. Plot a bifurcation diagram for r between 0 and 4
The bifurcation diagrams are shown in 4.1.3.

4.1.3 Bifurcation Diagram

To plot the bifurcation diagram, the main coding process is divided into two sequential loops. The first loop runs the number of iterations before plotting, to settle the data on the attractor. The second loop runs the number of iterations used for plotting, to indicate the data distribution on the attractor. The bifurcation diagram in Figure 7 plots the logistic map with two r ranges. As shown in 7a, the transcritical bifurcation occurs with $r = 1$, and the steady state of the system switches from $x^* = 0$ to $x^* = 1 - 1/r$. As shown in 7b, the system continues to keep the steady state of $x^* = 1 - 1/r$ until $r = 3$. Afterwards, the system follows the path to chaotic. Firstly, it transforms to a stable 2-cycle, then a 4-cycle, then an 8-cycle, and so on. The cycles are doubled with an accelerating rate. Eventually, the system is completely in chaos, and the system state is unpredictable. As shown in Figure 8 as a whole graph, the transfer between two subgraphs in Figure 7 is continuous and smooth, as there exists no bifurcation at $r = 2$.

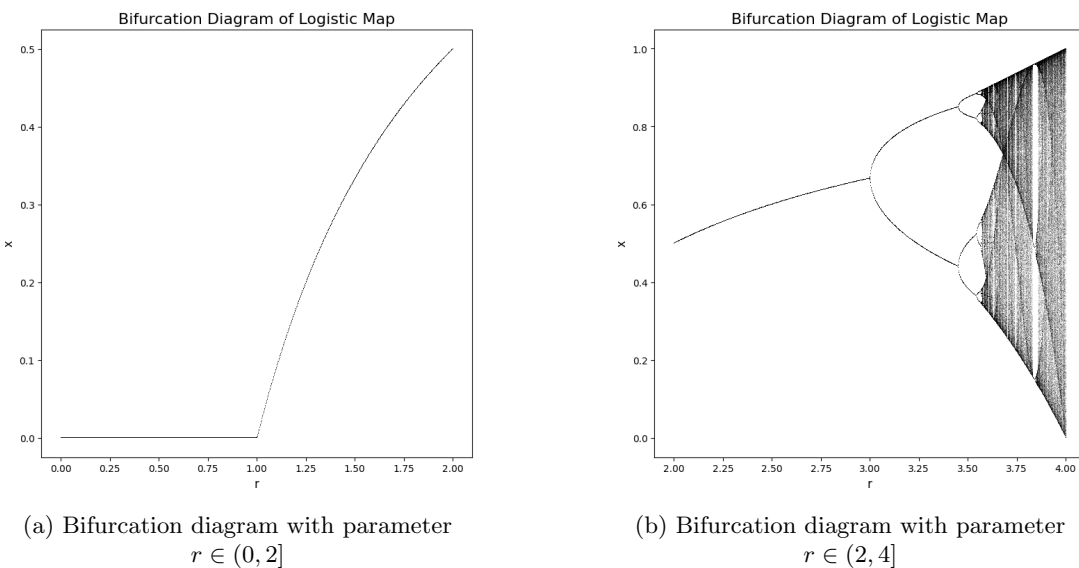


Figure 7: Bifurcation diagram of logistic map with different r ranges

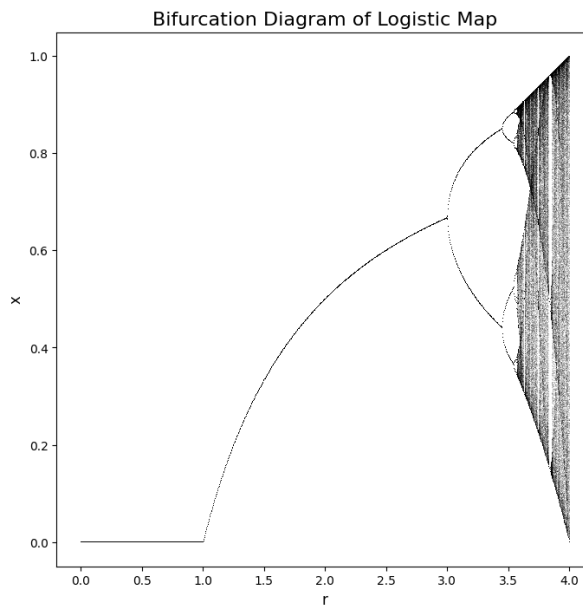


Figure 8: Overall bifurcation diagram of logistic map, $r \in (0, 4]$

4.2 Lorenz Attractor

The task is to analyze the Lorenz attractor by plotting trajectories with different ρ values and initial conditions.

4.2.1 The Lorenz Attractor

The Lorenz system originates from a simplification of atmospheric convection problems. The system is modeled via the following equations [3]:

$$X' = -\sigma X + \sigma Y, \quad (10)$$

$$Y' = -XZ + rX - Y, \quad (11)$$

$$Z' = XY - bZ. \quad (12)$$

where σ , r , and b are originally atmospheric parameters (In Lorenz's original paper, the parameters corresponding to r and b were denoted as r and b , respectively.). For the subsequent analysis, we use the following parameter values: $\sigma = 10$, $r = 28$, $b = 8/3$.

4.2.2 Visualized Trajectories with $\rho = 28$

The Lorenz system is encapsulated within a class, `Task42` in `dynamical_system.py`, whose responsibility is to implement the mathematical equations of the Lorenz system. Then, the `plot_lorenz` function in `utils.py` uses `solve_ivp` (solve initial value problem) in `scipy.integrate` to solve the ODE, and the solution of time as well as trajectory is returned. When running, an instance of the `Task42` class is created with a specific set of parameters, and then the calculation and the plotting are handled within `plot_lorenz`.

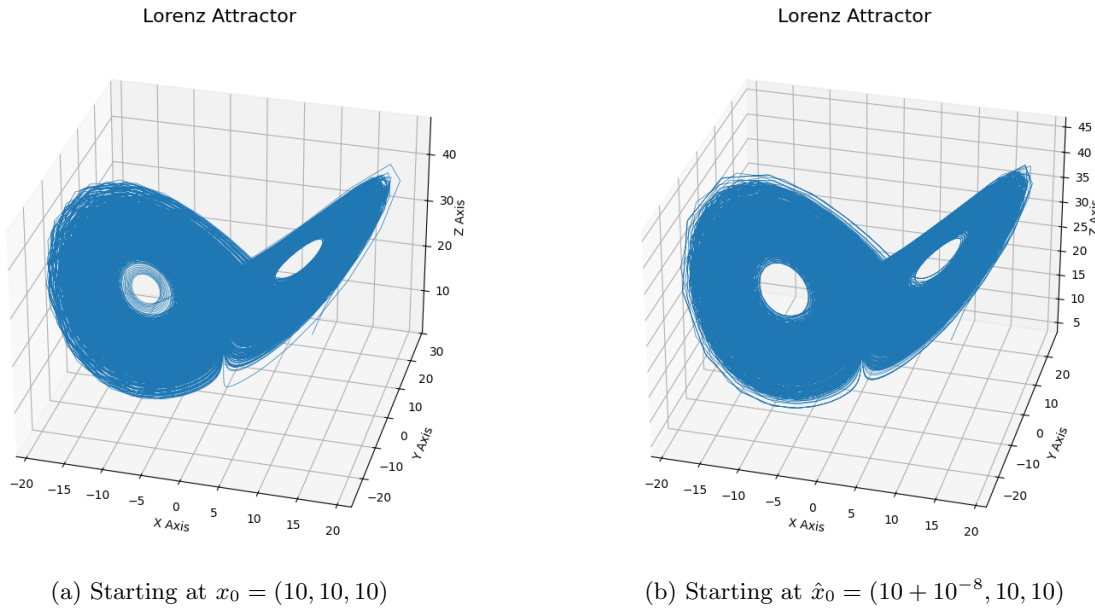
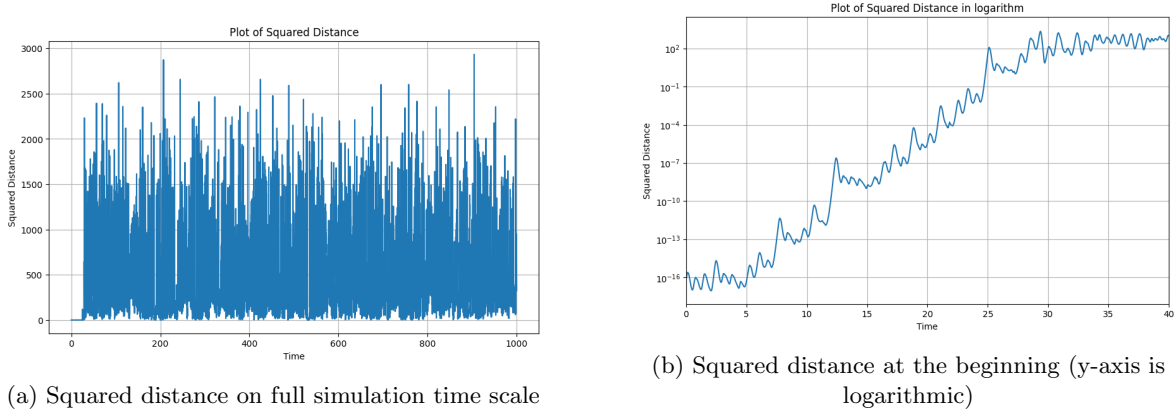


Figure 9: Single trajectory of the Lorenz system with $\rho = 28$

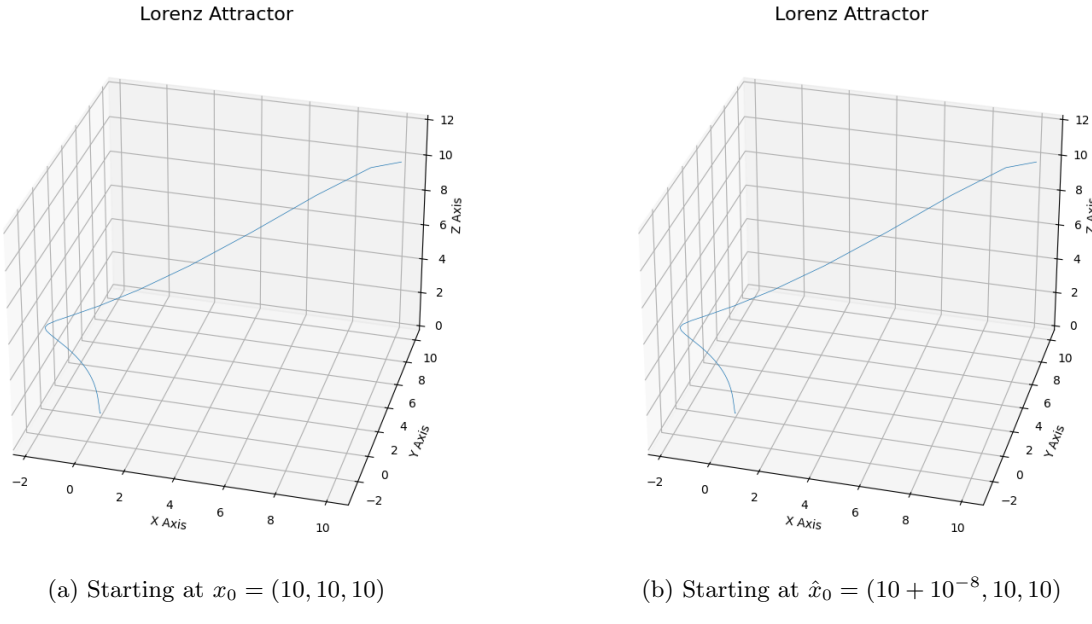
The simulation is set up with the following parameter values $\sigma = 10$, $r = 28$, and $b = 8/3$, with two initial conditions with minor differences. As shown in Figure 9, the classic Lorenz strange attractor starting at $x_0 = (10, 10, 10)$ has the shape of a two-lobed structure often likened to a butterfly's wings. Meanwhile, the sub-figure 9b shows that the trajectory with minor initial difference ($\hat{x}_0 = (10 + 10^{-8}, 10, 10)$) is mostly indistinguishable from the one in 9a.

Figure 10: Difference between two trajectories with $\rho = 28$

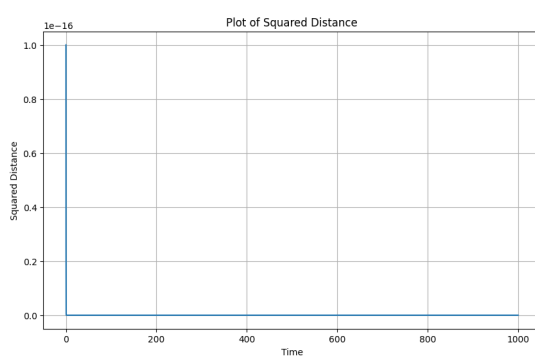
The Figure 10 plots the difference between two trajectories $\|x(t) - \hat{x}(t)\|^2$ against time. Figure 10a shows the distance over the full simulation time. From the figure, the difference fluctuates vastly from 0 to 3000, and the value is irregular. It shows that the trajectories have become totally uncorrelated with each other when observed on the full simulation time scale. The more detailed initial situation can be observed via Figure 10b, as the y-axis is logarithmic with time in $t \in [0, 40]$. The figure demonstrates an exponential growth of the squared difference for around $t \in [0, 30]$. By analyzing the simulation data, the difference between the points on the trajectory is larger than 1 at approximately $t = 25$. This shows that the trajectory of the Lorenz system is very sensitive to initial conditions, which is the primary characteristic of chaos.

4.2.3 Visualized Trajectories with $\rho = 0.5$

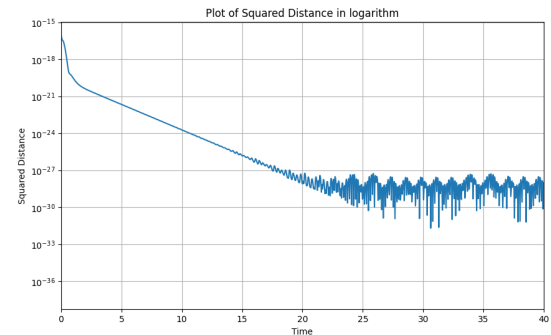
To verify bifurcation behavior, we run the same experiment with ρ changing from 28 to 0.5.

Figure 11: Single trajectory of the Lorenz system with $\rho = 0.5$

The simulation is set up with the following parameter values $\sigma = 10$, $\beta = 8/3$, and $\rho = 0.5$, with the same two initial conditions with minor differences. From Figure 11, we can observe that the system has only one fixed point at $(0, 0, 0)$, and the sub-figures 11a and 11b are visually indistinguishable from each other. It can be inferred from the figure that a bifurcation does happen. By $\rho = 28$, the system has a strange attractor, while by $\rho = 0.5$, the system has a single global fixed point. The two-phase portraits are clearly not topologically equivalent; therefore, a bifurcation occurred.



(a) Squared distance on full simulation time scale



(b) Squared distance at the beginning (y-axis is logarithmic)

Figure 12: Difference between two trajectories with $\rho = 0.5$

Similarly, the Figure 12 plots the difference between two trajectories $\|x(t) - \hat{x}(t)\|^2$ against time. Figure 12a shows the distance over the full simulation time, while Figure 12b demonstrates a more detailed initial situation as the y-axis is logarithmic with time in $t \in [0, 40]$. From the figure, the squared distance value at $t = 0$ is $1e^{-16}$, which is exactly the squared value of the initial difference $1e^{-8}$. Then the squared distance decreases almost instantly, and oscillates between around $1e^{-27}$ and $1e^{-24}$, which is barely observable on the full simulation time scale with a linear y-axis. Only in Figure 12b with a logarithmic y-axis can we see the squared distance decrease exponentially at the initial state.

5 Bifurcations in Crowd Dynamics

5.1 SIR Model Implementation and Code

To complete `sir_mode.py`, code and documentation additions had to be made. Firstly, the given functions to `us`, `mu`, `R0`, `h`, and `model` were properly documented with docstrings. These docstrings contain explanations of the functions, arguments, and return types. After this, the equations regarding the SIR model were put into the `model` function. These equations represent how susceptible (`S`), infected (`I`), and removed (`R`) variables change over time in the *continuous* implementation of the SIR model. The given and implemented equations are as follows:

$$\frac{dS}{dt} = A - \delta S - \frac{\beta SI}{S + I + R} \quad (11)$$

$$\frac{dI}{dt} = -(\delta + \nu)I - \mu(b, I)I + \frac{\beta SI}{S + I + R} \quad (12)$$

$$\frac{dR}{dt} = \mu(b, I)I - \delta R \quad (13)$$

The `model` function already included retrieval of the `S`, `I`, and `R` variables and had the $\mu(b, I)$ function results in variable `m`. Together with the remaining input variables to the function, the necessary formulas are given to `dSdt`, `dIdt`, and `dRdt`. In addition to this, to make the later parts of the task easier, plotting parts of the `task5.ipynb` file was moved to `sir_mode.py`. This was mostly done to create more modular code and make the change of parameter `b` in the next part easier to implement in the main task file.

The final version of the code plots three graphs for the first part of the task. This is done by the newly added `plot_continuous_SIR` function to `sir_mode.py` by carrying the plotting code from `task5.ipynb`. These graphs can be given in the Figure 13. The three plots are as follows:

- **Graph 1:** Susceptible (`S`), infected (`I`), and removed (`R`) over time.
- **Graph 2:** Comparison of Recovery rate and infected (`I`) variable over time.
- **Graph 3:** Indicator function value given infected (`I`) variable.

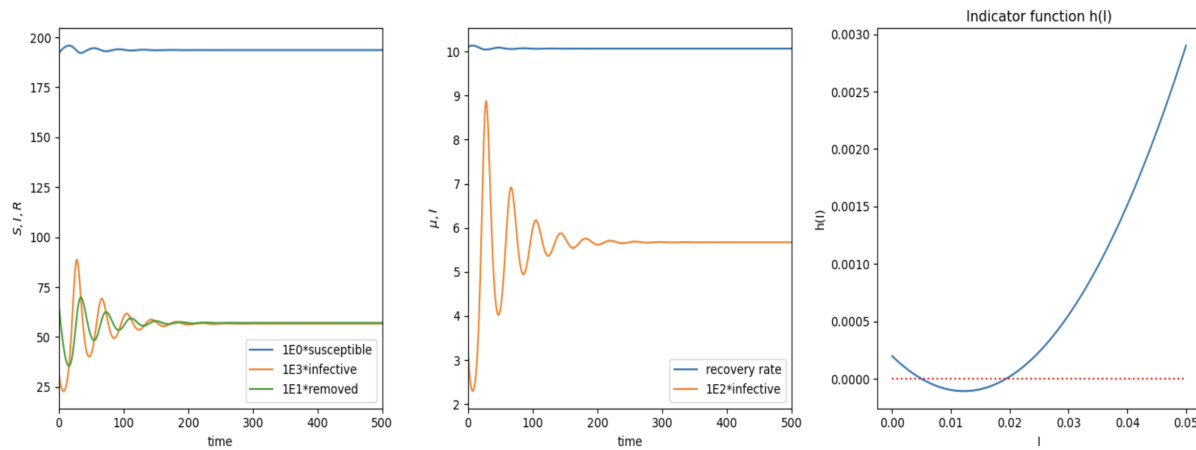


Figure 13: Different Graphs Plotted Regarding the SIR Model

5.2 Change of Parameter b

To observe the effects of parameter b on bifurcation, a loop with increments of 0.001 is created in the range $[0.01, 0.03]$; plotting 21 graphs in total. This loop is written in `sir_mode.py` and uses the function `plot_trajectories` that is created by carrying the plotting code. In each iteration, the new iteration value in the loop is assigned to b and the graph is plotted. For better plotting, NT value is upped to 15000, and scatter plots are commented out. Experimenting with different setups, this gave the best-looking figures. 9 figures out of the 21 plots are chosen to demonstrate the effect of changing the variable b , which can be seen in Figure 14. Since all the parameters are already set, only coloring the trajectories was left. RGB coloring was used for each starting point (S_0, I_0, R_0) .

- (195.3, 0.052, 4.4): Red
- (195.7, 0.03, 3.92): Green
- (193, 0.08, 6.21): Blue

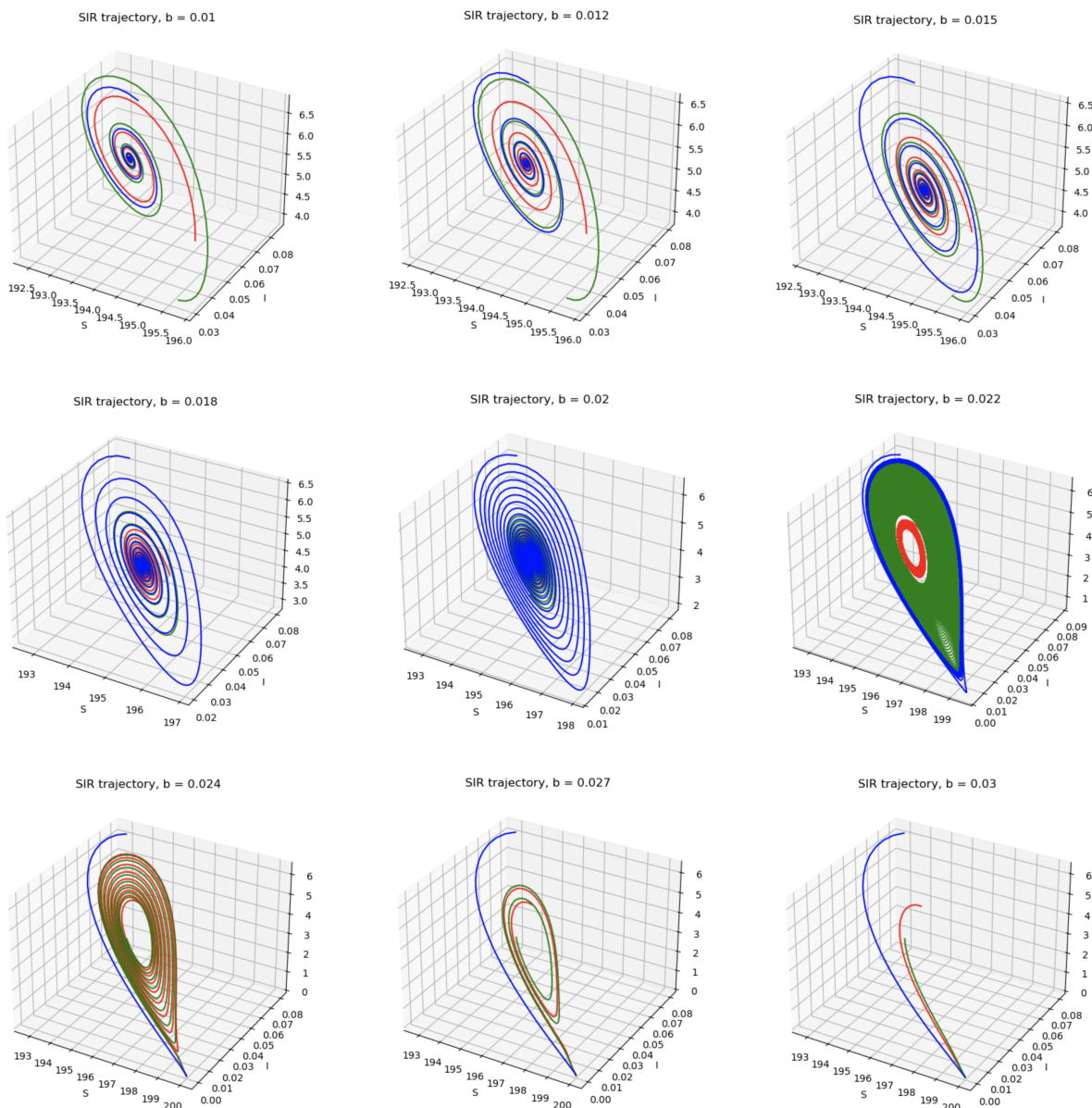


Figure 14: Trajectories of the SIR model with varying b values.

5.3 Bifurcation Analysis

Analyzing the trajectories, it can be seen that bifurcation happens exactly at the point $b = 0.022$, which is a **Hopf Bifurcation**. System of equations describing the normal form of the bifurcation can be found in [2], and is given as

$$\dot{x}_1 = \alpha x_1 - x_2 - x_1(x_1^2 + x_2^2), \quad (14)$$

$$\dot{x}_2 = x_1 + \alpha x_2 - x_2(x_1^2 + x_2^2). \quad (15)$$

The **Hopf Bifurcation** can be devised when a stable fixed point becomes unstable, so instead of the system settling into a single point, it oscillates forever around it. This is exactly what occurs at $b = 0.022$ as can be seen from the figure. After this point, a stable limit cycle comes. The analysis of the trajectories for all values of b between $[0.01, 0.03]$ can be generalized as follows:

- $b < 0.022$: All three trajectories spiral towards a stable fixed point, an attractor. This shows a stable equilibrium for all given initial points. In the model sense, the value of b is small enough that the system stabilizes after some oscillation, meaning the epidemic reaches a steady state over time, and the infection settles into a non-changing number of infected people.
- $b = 0.022$: The spiraling convergent behavior gives its place to a forever oscillating behavior, meaning at this exact value, the stable point becomes unstable and a limit cycle emerges. As said before, the system oscillated forever rather than settling into a single point. This limit cycle (closed-loop trajectory) becomes the new attractor.
- $b > 0.022$: Similar to the $b < 0.022$ case, the system converges to a stable fixed point again. This time, the point is around $(200, 0, 0)$ for the S, I, and R variables. This also happens to be the state with no infected people.

5.4 Reproduction Rate

The reproduction rate (R_0) is defined in [4] and given by:

$$R_0 = \frac{\beta}{d + \nu + \mu_1} \quad (16)$$

The variables used for the equation are given as:

- β : Average number of adequate contacts per unit time with infectious individuals.
- d : Per capita natural death rate.
- ν : Per capita disease-induced death rate.
- μ_1 : Maximum recovery rate based on the number of available beds.

R_0 measures how many new infections one infected person can generate, accounting for the ways to stop the spread, death rates, and hospitalization (recovery). Since β is in the numerator, increasing and decreasing it will have the same effect on R_0 . When β is increased, R_0 also increases; causing more secondary infections. The number of infected people will therefore likely increase. On the contrary, decreasing the β decreases R_0 ; meaning each infected person will cause fewer new infections. Though the infection may still spread, the effect of it through secondary people diminishes, causing the infection to die out or at least cause the infective people to decline over time. $R_0 = 1$ is an obvious cut-off for the behavior change of the infection. The further R_0 is above 1, the faster the infection spreads; the further it is below 1, the more rapidly the infection dies out.

5.5 Attracting Node and E_0

In [4], it's stated in 3.2 that for the system (2.2), the disease-free equilibrium E_0 is an attracting node when $R_0 < 1$. This means that when the recovery rate is smaller than 1, the starting SIR points (S_0, I_0, R_0) that are close to E_0 will reach this steady equilibrium state, and the system will stay there. This is a free-disease state, as the infected people are 0, meaning the infection won't spread through the population. The analysis in Figure 14 shows this clearly as for $b > 0.022$, the system reaches the equilibrium point since $A = 20$, and $d = 0.1$.

$$E_0 = \left(\frac{A}{d}, 0, 0 \right) = \left(\frac{20}{0.1}, 0, 0 \right) = (200, 0, 0) \quad (17)$$

5.6 Bonus: Analysis of Another Type of Bifurcation

In the original paper by Shan and Zhu (2014) [4], the authors analyze the bifurcation structure of an extended SIR model in which the recovery rate depends on the number of available hospital beds per capita, represented by the parameter b . Based on this setup, the authors identify a critical value of b given by

$$b_c = \frac{A(\mu_1 - \mu_0)}{\beta(\beta - \nu)} \quad (18)$$

at which the system is expected to exhibit a *pitchfork bifurcation*, and transitions between forward and backward bifurcation regimes depending on parameter values.

5.6.1 Experiment 1

To numerically investigate this claim, we fixed the model parameters as follows: $A = 20$, $\delta = 0.1$, $\nu = 1.0$, $\mu_0 = 10$, $\mu_1 = 10.5$, and chose the transmission rate $\beta = 11.6$ such that the basic reproduction number becomes exactly

$$\mathcal{R}_0 = \frac{\beta}{\delta + \nu + \mu_1} = 1 \quad (19)$$

This ensures that we are operating precisely at the bifurcation threshold, as assumed in the theoretical analysis. We then varied b between 0.01 and 0.09 in small increments and numerically solved the ODE system using a stiff solver with strict tolerances to ensure qualitative correctness.

Our simulations aimed to observe the qualitative behavior of the system and identify the bifurcation type as b crosses the critical threshold. For small values of b , the trajectories exhibit damped oscillations that converge to a non-zero endemic equilibrium, consistent with *backward bifurcation* where multiple steady states may coexist. As b increases and surpasses $b_c \approx 0.074$, trajectories from various initial conditions converge directly to a unique equilibrium, indicating a transition to *forward bifurcation* behavior.

However, contrary to the theoretical expectation of a pitchfork bifurcation at the critical b , our simulations do not show any evidence of symmetric splitting or the emergence of multiple new equilibria from a central one. This suggests that, under the fixed parameter set (especially the choice of β and μ_1 to ensure $\mathcal{R}_0 = 1$), the system does not satisfy the additional conditions necessary for a pitchfork bifurcation to manifest visually or dynamically. This highlights the sensitivity of the bifurcation structure to parameter configurations and reinforces the importance of numerical validation in nonlinear epidemiological models.

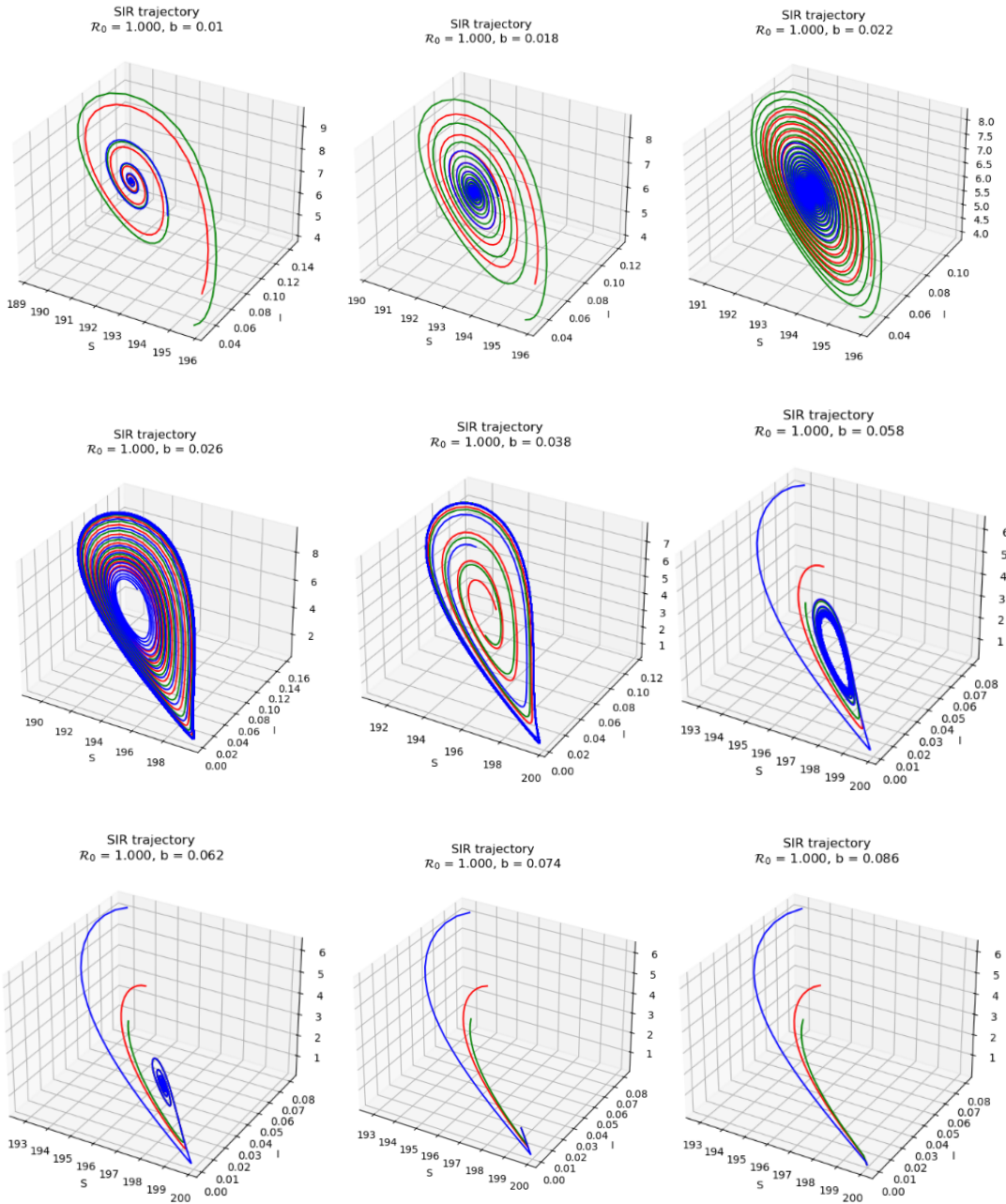


Figure 15: SIR model trajectories for varying values of b between 0.01 and 0.09, while keeping $\mathcal{R}_0 = 1$

The Figure 15 illustrates the qualitative change in the system's behavior: for low values of b (e.g., $b = 0.01$), trajectories spiral toward a stable endemic equilibrium, indicating a backward bifurcation regime. As b increases (e.g., $b = 0.058, 0.062$), the spiral becomes tighter and the system approaches the threshold. For b values beyond the critical threshold (e.g., $b = 0.074$ and higher), trajectories converge monotonically to a unique disease-free equilibrium (E_0).

5.6.2 Experiment 2

The Shan–Zhu SIR model with dynamic recovery rate $\mu(b, I)$ exhibits several codimension-1 bifurcations [4].

Here we focus on the forward transcritical bifurcation that occurs when the disease-transmission parameter β crosses the threshold $\beta_c = d + \nu + \mu_1$. We will give a numerical illustration and discuss it below.

The disease-free equilibrium $E_0 = (A/d, 0, 0)$ is stable for $R_0 < 1$ and loses stability at $R_0 = 1$. Where endemic equilibrium $E_1(\beta)$ emerges, the textbook signature of a **transcritical** bifurcation.

Parameter set is given below:

$$A = 20, d = 0.1, \nu = 1, \mu_0 = 10, \mu_1 = 10.45, b = 0.01, \beta \in \{9.0, 11.55, 13.0\}. \quad (20)$$

The initial condition $(S, I, R) = (195, 0.05, 5)$ is identical for all runs.

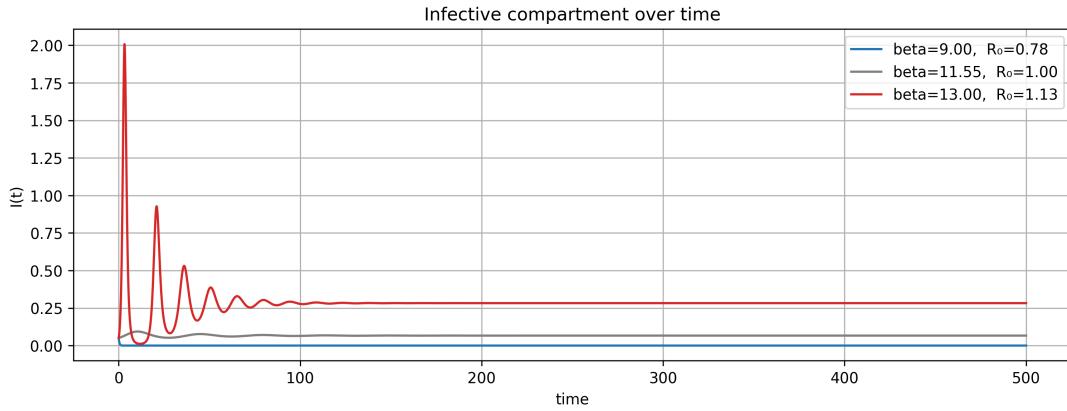


Figure 16: Trajectories of $I(t)$ for three representative values of β (below, at, and above the threshold β_c).

The figure 16 shows that $I(t)$ decays to zero for $R_0 < 1$, stagnates marginally at $R_0 = 1$. And approaches a positive level for $R_0 > 1$.

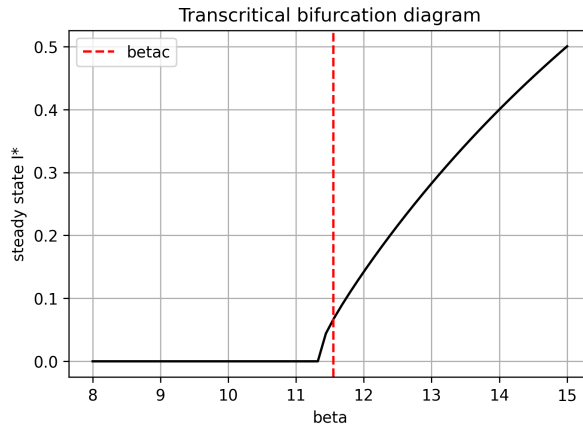


Figure 17: Forward transcritical bifurcation at $\beta_c = 11.55$. Solid lines: stable; dashed: unstable.

Figure 17 suggests that the endemic equilibrium attracts nearby trajectories for $\beta > \beta_c$.

Crossing $R_0 = 1$ changes the sign of the eigenvalue associated with the infected manifold. No limit cycles are created or destroyed; the qualitative change is confined to the fixed-point structure, matching the normal form $\dot{x} = \alpha x - x^2$.

A single-parameter sweep in β suffices to reveal a clear transcritical bifurcation in the Shan–Zhu model, from our observations, validating the analytical prediction.

References

- [1] T.W. Gamelin and R.E. Greene. *Introduction to Topology*. Dover books on mathematics. Dover Publications, 1999. URL: <https://books.google.de/books?id=thAHAGyV2MQC>.
- [2] Yuri A. Kuznetsov. *Elements of Applied Bifurcation Theory*. Springer, New York, 2004.
- [3] Edward N. Lorenz. Deterministic nonperiodic flow. *Journal of Atmospheric Sciences*, 20(2):130 – 141, 1963. URL: https://journals.ametsoc.org/view/journals/atsc/20/2/1520-0469_1963_020_0130_dnf_2_0_co_2.xml, doi:10.1175/1520-0469(1963)020<0130:DNF>2.0.CO;2.
- [4] Chunhua Shan and Huaiping Zhu. Bifurcations and complex dynamics of an sir model with the impact of the number of hospital beds. *Journal of Differential Equations*, 257(5):1662–1688, September 2014.
- [5] S.H. Strogatz. *Nonlinear Dynamics and Chaos: With Applications to Physics, Biology, Chemistry, and Engineering*. Chapman and Hall/CRC, 3rd edition, 2024. doi:10.1201/9780429398490.
- [6] Steven H. Strogatz. *Nonlinear Dynamics and Chaos*. Westview Press, 2001.